Published in final edited form as:

Nat Struct Mol Biol. 2010 March ; 17(3): 289–293. doi:10.1038/nsmb.1755.

The structures of the anti-tuberculosis antibiotics viomycin and capreomycin bound to the 70S ribosome

Robin E. Stanley[1,2,*], **Gregor Blaha**[1,*], **Robert L. Grodzicki**[1,3], **Michael D. Strickler**[1,3], and **Thomas A. Steitz**[1,3,4]

[1]Department of Molecular Biophysics and Biochemistry, Yale University, New Haven, CT 06520, USA

[3]Howard Hughes Medical Institute, New Haven, CT 06520, USA

[4]Department of Chemistry, Yale University, New Haven CT 06520, USA

Abstract

Viomycin and capreomycin belong to the tuberactinomycin family of antibiotics, which are among the most effective antibiotics against multidrug-resistant tuberculosis. Here we present two crystal structures of the 70S ribosome complexed with three tRNAs and bound to either viomycin or capreomycin at 3.3 and 3.5 Å resolution, respectively. Both antibiotics bind to the same site on the ribosome, which lies at the interface between helix 44 (h44) of the small ribosomal subunit and Helix 69 (H69) of the large ribosomal subunit. The structures of these complexes suggest that the tuberactinomycins inhibit translocation by stabilizing the tRNA in the A site in the pre-translocation state. In addition these structures show that the tuberactinomycins bind adjacent to the paromomycin and hygromycin B antibiotics, which may enable the development of new derivatives of tuberactinomycins that are effective against drug resistant strains.

Introduction

Despite modern multidrug therapy 1 and ongoing drug development 2,3, tuberculosis (TB) continues to be a major health concern with nine million new cases and two million deaths worldwide in 2007 alone 4, which makes the emergence of strains of *Mycobacterium tuberculosis*, the causative agent of TB, that are resistant to the most widely used antibiotics a significant health problem. Among the most effective antibiotics against multidrug-

Correspondence to: Thomas A. Steitz thomas.steitz@yale.edu.

[2]Present address: Laboratory of Molecular Biology, NIDDK, NIH, Bethesda, Maryland 20892, USA.

[*]These authors contributed equally to this work

Author Contributions: R.E.S. prepared and crystallized the complexes; R.E.S. and G.B. collected data, processed and refined X-ray data; G.B. and R.L.G. purified all components of complex; M.D.S. energy minimized the initial tuberactinomycin structures and solved all computational problems related to large size of the datasets and of the complexes; T.A.S, G.B. and R.E.S. contributed to the experimental design and analysis of the structure; T.A.S, G.B. and R.E.S. wrote the manuscript, on which all authors commented.

Accession Codes: Atomic coordinates for both copies of the 70S ribosome in the asymmetric unit of both tuberactinomycin complexes have been deposited in the Research Collaboratory for Structural Bioinformatics Protein Data Bank with accession numbers 3KNH, 3KNI, 3KNJ, and 3KNK for viomycin bound 70S ribosome structure, and 3KNL, 3KNM, 3KNN, and 3KNO for capreomycin bound 70S ribosome structure.

resistant TB are the tuberactinomycins. The tuberactinomycins inhibit protein synthesis by interacting with both ribosomal subunits in a manner that was unknown until the present study 5.

The tuberactinomycin family of antibiotics consists of several closely related compounds containing the same pentapeptide core that is composed of L-serine and the nonproteinogenic amino acids 2,3-diaminopropionate, L-capreomycidine, and β-ureidodehydroalanine (Fig. 1). The members of the tuberactinomycin family differ in their amino acid side chain modifications, including the amino acylation with β-lysine 6. Although viomycin was the first member of this family to be identified, only capreomycin is commonly used clinically as a second-line antibiotic against infections by *Mycobacterium tuberculosis* 7. Capreomycin is a mixture of four isoforms, all of which are active *in vitro* against mycobacteria 8. To simplify the discussion here, only the IA isoform of capreomycin is considered (Fig. 1); other isoforms either are not modified with β-lysine and/or have the serine of the cyclic pentapeptide core reduced to alanine (Supplementary Fig.1).

In addition to its important role in the treatment of TB, viomycin has played a pivotal role in biochemical studies of protein synthesis. Viomycin interacts with both the large and the small ribosomal subunits 5 and prevents the translocation of the ribosome along the mRNA 9. During translocation, a deacylated tRNA moves from the P site to the E site and the peptidyl-tRNA moves from the A site to the P site to vacate the A site for the next aminoacylated tRNA. Elongation Factor G (EF-G) facilitates translocation using GTP hydrolysis. Although, viomycin allows the binding of EF-G and GTP hydrolysis, it completely inhibits translocation 9. To confirm the proposed binding site and illuminate the mechanism of translocation inhibition we set out to determine the structure of both capreomycin and viomycin bound to the ribosome.

Results

The co-crystal structures of the 70S ribosome from *Thermus thermophilus* complexed with either viomycin or capreomycin as well as three full length tRNAs and a short piece of mRNA were determined at 3.3 and 3.5 Å resolution, respectively. Both antibiotics were bound to *T. thermophilus* 70S ribosomes that had been complexed with mRNA and tRNA prior to crystallization. The preparation of ribosomes containing the 3 bound tRNAs required the incubation with the ternary complex of EF-Tu, GMP-PNP and Gln-tRNA^{Gln} (see methods). Unbiased difference Fourier maps were calculated using the observed amplitudes from crystals of the complex and the amplitudes and phases that were calculated using a model of the 70S ribosome without the bound ligands obtained by molecular replacement. Each antibiotic as well as the tRNA and mRNA could be manually fit into the difference electron density map (Fig. 1c), and the coordinates of the entire ribosome complex with the antibiotic, tRNAs and mRNA were then refined. The distinctive axial conformation of the six membered ring of the L-capreomycidine side chain allowed the central tuberactinomycin ring to be unambiguously placed into the difference Fourier maps, despite the presence of the four isoforms of capreomycin.

The three tRNA molecules are bound in the classical A, P and E sites in this complex with the 70S ribosome. The anticodons of both the A-site and the P-site tRNAs form base-pairs with the corresponding codons of the mRNA. As observed earlier 10, the bases A1492 and A1493 make stabilizing A-minor interactions with the two base-pairs between the codon and anti-codon of the A-site tRNA and mRNA. The structure of peptidyl transferase center and the bound CCA ends of both the A-site and P-site tRNAs is identical to that of the *Haloarcula marismortui* large subunit complexed with A- and P-site substrate analogues 11, consistent with the recent results of Ramakrishnan and colleagues 12 (Supplementary Fig. 2).

Both viomycin and capreomycin bind to a site that lies between the large and small subunit in a cleft formed between helix 44 of the 16S rRNA (h44) and the tip of Helix 69 of 23S rRNA (H69)(Fig. 2). The macrocycle of both drugs lies within hydrogen bonding distance of the ribose-phosphate backbone of the binding pocket, which is formed by residues A1913 and C1914 of the 23S rRNA and residues A1493 and G1494 of the 16S rRNA. This explains why cleavage of the phosphate backbone between A1493 and G1494, produced by colicin E3, renders the ribosome less sensitive to inhibition by viomycin 13. The orientation of the macrocycle is also determined by its stacking onto the base of G1491 and G1494, which places the six membered ring of the capreomycidine side chain in the vicinity of the bases of A1492 and A1493 of the 16S rRNA. The guanidinium moiety in the six membered ring of capreomycidine effectively positions the antibiotic by making a salt bridge to the phosphate of A1493 of the 16S rRNA (Fig. 2c). Previous biochemical work has established the importance of the capreomycidine side chain of the tuberactinomycins ring for its inhibition of the ribosome activity, suggesting that its steric restriction of the orientation of A1492 and A1493 contributes to the inhibitory effect of viomycin and capreomycin 14; A1492 and A1493 cannot move to the positions they occupy in the *apo*-ribosome in the presence of these antibiotics.

The main difference between the binding of viomycin and capreomycin to the 70S ribosome is in the β-lysine side chain of each drug. Because only 2 of the 4 isoforms of capreomycin possess the β-lysine modification, the electron density observed for β-lysine in the complex between capreomycin and the ribosome is weak. The β-lysine side chain in the capreomycin complex extends from the macrocycle, past A1913 of the 23S rRNA and towards the A-site tRNA, while in the viomycin complex it extents past G1491 of the 16S rRNA towards the mRNA. Neither position of the β-lysine modification is essential for the activity of the antibiotic 15,16, which is confirmed by the lack of extensive hydrogen bonding between the ribosome and the modification.

Discussion

The structures of both viomycin and capreomycin bound to the ribosome confirm a wealth of previous biochemical and genetic studies which suggested that the tuberactinomycins bind at the interface between the small and large ribosomal subunits. Both tuberactinomycins bind to the well conserved intersubunit bridge B2a formed by the interactions of H69 of the 23S rRNA and h44 of the 16S rRNA. Mutations of nucleotides in both H69 and h44 that surround the antibiotic binding site, confer resistance to capreomycin

and viomycin 17. The loss of 2' methylation of C1409 of h44 and C1920 of H69 reduces the susceptibility of *Mycobacterium tuberculosis* to capreomycin and viomycin by two to eightfold 7 but has no effect on capreomycin sensitivity in *T. thermophilus* 17. Of particular interest is the mutation A1913U, which was identified in *T. thermophilus* 17. In the structure of the *apo* 70S ribosome the base of A1913 is swung out of the loop at the base of H69 and inserted into h44 18, a position which partially overlaps with the binding site of both capreomycin and viomycin. The mutation of A1913 to U may confer resistance to these antibiotics because this potential clash between A1913 and the antibiotic could be alleviated, which also suggests that bound tuberactinomycins inhibit translocation by preventing A1913 from moving into the position it occupies in the structure of the *apo* 70S-ribosome.

The bridge between the subunits formed by H69 and h44 is not only essential for the association of ribosomal subunits in the absence of tRNA 19, but also contacts the A-site tRNA implying that it has roles in several ribosomal functions such as initiation, decoding, or ribosome recycling 20–22. Several different orientations of this bridge have been observed in the crystal structures of ribosome complexes with tRNAs, release factors and antibiotics 18,22–28. The positions of A1913 of the 23S rRNA as well as A1492 and A1493 of the 16S rRNA play a critical role in the decoding of the mRNA. The positions of A1492, A1493, and A1913 in the structures presented here are identical to those observed with complexes containing mRNA and cognate tRNA in the A site 10,24. During the binding of the cognate A-site tRNA, the nucleotides A1492 and A1493 swing out of h44 and, along with G530 of the 16S rRNA, form A minor interactions with the helix that is formed by the codon:anticodon interactions between the cognate tRNA and the mRNA 10. In addition, A1913 rotates towards the A-site tRNA to hydrogen bond with the 2'-OH of nucleotide 37 of the A-site tRNA 24.

Chemical modification experiments 29 and cryo-EM structures 30 show that the tRNAs can assume a hybrid state, in which the tRNAs bound in the A site and P site adopt the A/P and P/E hybrid states, respectively, after the peptidyl transfer reaction. There are reports on the effects of viomycin on these hybrid states, which are not in agreement with each other. These disagreements might just be the consequence of the differing ionic conditions used on these experiments, which could influence the sensitive equilibrium between the two states 30,31. Single molecule-FRET experiments suggest that viomycin not only stabilizes the classical state, but also suppresses the rate of sampling the hybrid state by the tRNAs after peptide bond formation 31. Other kinetic data suggest that the binding of viomycin to the 70S ribosome after the addition of EF-G and GTP blocks only the movement of the A-site tRNA but not the formation of the hybrid state by the P-site tRNA 32. Chemical modification experiments seem to indicate that viomycin traps the tRNAs in the A/P and P/E hybrid state 33. Single molecule FRET experiments 34 have correlated both the tRNA hybrid state and the viomycin stalled state with the ratcheted state of the ribosome, in which the large subunit is rotated relative to the small and tRNAs. While we cannot confirm or refute the possibility that these antibiotics bind to the 70S ribosome in the hybrid state, our results show that they can bind to the classical state.

In both structures of the ribosome in complex with viomycin and capreomycin, the ribosome is observed in the non-ratcheted with the bound tRNAs in the classical A, P and E sites

rather than in the ratcheted state with the bound tRNA in the hybrid state. Crystal packing and/or the presence of an E-site tRNA in these crystals may prevent the formation of the hybrid state. Although, these structures demonstrate that viomycin is able to bind to the ribosome when the A-site tRNA is in the classical state, we cannot exclude the possibility that viomycin is capable of binding to the ratcheted state as well. Cryo-EM structures have revealed that bridge B2a, which is consists of h44 and H69, remains intact after spontaneous ratcheting of the subunits, however slight movements of h44 and H69 were observed 30. This is further supported by recent crystals structures of the 70S ribosome from *E. coli* captured in intermediate states of ratcheting, which show that the contacts in B2a persist in the different proposed intermediate states 35. Whether or not the binding of viomycin inhibits the movement of B2a that is associated with ratcheting is unknown.

The many different classes of antibiotics that affect translocation of the tRNAs on the ribosome, such as the tuberactinomycins or aminoglycosides (Reviewed in 36) either stabilize the tRNA in the pre-translocation state or interfere with the conformational changes of the ribosome or tRNA required for translocation 37. Paromomycin is an aminoglycoside that binds into the major groove of h44 and stabilizes A1492 and A1493 of the 16S rRNA in the flipped out position that the bases adopt during the readout interaction between the tRNA anticodon and the mRNA 10. Because paromomycin stabilizes the binding of both cognate and near-cognate tRNAs to the A site, it not only inhibits translocation but also promotes miscoding 38. Interestingly, although hygromycin B also binds to h44, it causes only the base of A1493 to adopt a unique orientation, in which the base interferes with the movement of the tRNA from the A site to the P site 39.

Viomycin and capreomycin not only affect the positioning of the bases of A1492 and A1493 (Fig. 3), but they also appear to affect the position of A1913 of the 23S rRNA. The base of A1913 adopts a position where it forms hydrogen bonds with the A-site tRNA. Consistent with our results is the biochemical evidence that viomycin increases the affinity of tRNA to the A site by 1000 fold 37 and promotes the back translocation of the complex of tRNA with mRNA on the ribosome 40. Therefore we propose that the tuberactinomycins inhibit translocation stabilizing the tRNA in the A-site.

We suggest that these two structures of tuberactinomycins in complex with the 70S ribosome will enable the creation of new anti-TB antibiotics. The tuberactinomycins have several functional groups that can be modified without decreasing the potency of their inhibition of translation making them particularly amenable for structural based drug design 16. Furthermore, the adjacent location of the tuberactinomycin binding site with those of paromomycin and hygromycin should provide an enabling starting point for the design of novel derivatives of tuberactinomycins that are chemically linked to modified portions of the other antibiotics. These new compounds could be effective against drug resistant strains of TB, including those with mutant efflux pumps.

Methods

Purification of 70S ribosomes, mRNA, tRNA, and ternary complex

Thermus thermophilus 70S ribosomes and fMet-tRNA were prepared as described previously 24,41,42. The mRNA was chemically synthesized by Integrated DNA Technologies (Coraliville, IA) and contained a codon for Gln following the fMet start codon. The ternary complex of EF-Tu, Gln-tRNA^{Gln} and GMP-PNP was formed from purified components. The plasmids for the overexpression of His-tagged T.th. EF-Tu and His-tagged T.th. EF-Ts were provided by Poul Nissen and Mathias Sprinzl, respectively. Both EF-Tu and EF-Ts were expressed and purified following standard protocols. tRNA^{Gln} and Gln-RS were prepared as described previously 43. Prior to ternary complex formation with Gln-tRNA^{Gln}, the nucleotide bound to EF-Tu was exchanged to GMP-PNP. The final ternary complex was purified with a reverse ammonium sulfate gradient on a phenyl resource column (GE, Piscataway, NJ).

Formation of the 70S ribosome complex

The complex of 70S ribosomes with viomycin (or capreomycin), mRNA and three tRNAs was formed in 5 mM Hepes- KOH (pH 7.6), 10 mM $MgCl_2$, 50 mM KCl, 10 mM NH_4Cl at 55°C. 4 μM of 70S ribosomes were programmed with 8 μM mRNA for 15 minutes, before incubating with 8 μM of fMet-tRNA$_i^{Met}$ for an additional 30 minutes. 16 μM of ternary complex was added to the reaction mixture and incubated for 30 minutes followed by the addition of either 100 μM of viomycin or 250 μM capreomycin and a final incubation of 30 minutes. The complex was cooled to room temperature and briefly centrifuged prior to setting up the crystallization experiment.

Crystallization

Crystals were grown by vapor diffusion in hanging drop crystallization trays, in which 1–2 μL of the ribosome complex was mixed with 1–2 μL of the reservoir solution that contained: 0.1–0.2 M Arginine-HCl, 0.1 M Tris-HCl (pH 7.6), 2.5%(w/v) PEG 20K, 7–12%(v/v) MPD, 0.5 mM BME. Within 2–5 days crystals of 50 × 100 × 1000 μm in size appeared. The crystals were stabilized by slowly increasing the concentration of MDP to a final concentration of 30%(v/v) before flash freezing in liquid nitrogen.

Data Collection

Xray diffraction data were collected at beamlines X29 at Brookhaven National Laboratory (Upton, NY) and 24ID at the Advanced Photon Source (Argone, IL). Complete datasets for both the viomycin and capreomycin crystals were collected from four separate regions of the same crystal. The raw data were integrated and scaled with the XDS package 44. The crystals belong to the orthorhombic spacegroup $P2_12_12_1$ with two copies of the ribosomal complex in the asymmetric unit.

Structure Determination

Each structure was solved by molecular replacement using the small and large ribosomal subunits from the structure of the *T. th.* 70S ribosome bound to mRNA and tRNA (PDB

ID's 2J00 and 2J01) using phaser in the CCP4 programming suite 45. Neither the tRNAs nor the mRNA ligands were included in the search models. The initial molecular replacement structures were refined by rigid body refinement with the ribosome split into multiple domains using REFMAC in the CCP4 programming suite 46. After rigid body refinement in REFMAC5 each structure was refined using Phenix, which enabled the calculation of difference electron density maps using Fo-Fc coefficients 47. Clear difference electron densities were visible for 3 full length tRNAs, the mRNA, and both antibiotics, which were used for building the ligands.

Structure Building

Iterative rounds of model building and refinement were carried out in Coot 48 and CNS 49,50. While the crystal structure of viomycin was reported in the literature 51 the coordinates are not available in the Cambridge Structural Database. The initial coordinates of viomycin and capreomycin were based on the combination of a model derived from the published crystal structure of tuberactinomycin 52, chemical structure information and energy minimization with the program Desmond 53. Initial structures were energy minimized using OPLS-AA force field 54 and TIP4P water model 55 via steepest descent / L-BFGS, followed by 1.2 ps of five-stage simulated annealing (0, 300K, 600K, 900K, 300K), and another cycle of energy minimization. The starting coordinates for the tRNA and mRNA ligands were taken from (PDB ID 2WGK 12). The deacylated non-cognate tRNA bound in the E-site was build with the same sequence as the A-site $tRNA^{Gln}$. The statistics on the X-ray data and the refinement are available in Table 1. Figures were generated with PYMOL 56.

Supplementary Material

Refer to Web version on PubMed Central for supplementary material.

Acknowledgements

We thank the staffs at the Advanced Photon Source beamline 24-ID and at the National Synchrotron Light Source beamline X29 for help during data collection and the staff at the Center for Structural Biology at Yale University for computational support. We also thank Ivan Lomakin for providing us with methionyl-tRNA synthetase, U.L. RajBhandary and K.H. Nierhaus for the overexpression plasmids of methionyl-tRNA formyltransferase and the initiator tRNA respectively. This work was supported by the US National Institutes of Health grant GM 22778 to T.A.S..

References

1. Guy ES, Mallampalli A. Managing TB in the 21st century: existing and novel drug therapies. Ther Adv Respir Dis. 2008; 2:401–408. [PubMed: 19124385]
2. Hugonnet JE, Tremblay LW, Boshoff HI, Barry CE 3rd, Blanchard JS. Meropenem-clavulanate is effective against extensively drug-resistant Mycobacterium tuberculosis. Science. 2009; 323:1215–1218. [PubMed: 19251630]
3. Makarov V, et al. Benzothiazinones kill Mycobacterium tuberculosis by blocking arabinan synthesis. Science. 2009; 324:801–804. [PubMed: 19299584]
4. WHO. Global Tuberculosis Control: Epidemology, Strategy, Financing: WHO report 2009. Geneva, Switzerland: World Health Organization; 2009. p. 314
5. Yamada T, Mizugichi Y, Nierhaus KH, Wittmann HG. Resistance to viomycin conferred by RNA of either ribosomal subunit. Nature. 1978; 275:460–461. [PubMed: 211438]

6. Thomas MG, Chan YA, Ozanick SG. Deciphering tuberactinomycin biosynthesis: isolation, sequencing, and annotation of the viomycin biosynthetic gene cluster. Antimicrob Agents Chemother. 2003; 47:2823–2830. [PubMed: 12936980]
7. Johansen SK, Maus CE, Plikaytis BB, Douthwaite S. Capreomycin binds across the ribosomal subunit interface using tlyA-encoded 2'-O-methylations in 16S and 23S rRNAs. Mol Cell. 2006; 23:173–182. [PubMed: 16857584]
8. Herr EB Jr, Redstone MO. Chemical and physical characterization of capreomycin. Ann N Y Acad Sci. 1966; 135:940–946. [PubMed: 5220248]
9. Modolell J, Vazquez. The inhibition of ribosomal translocation by viomycin. Eur J Biochem. 1977; 81:491–497. [PubMed: 202460]
10. Ogle JM, et al. Recognition of cognate transfer RNA by the 30S ribosomal subunit. Science. 2001; 292:897–902. [PubMed: 11340196]
11. Schmeing TM, Huang KS, Strobel SA, Steitz TA. An induced-fit mechanism to promote peptide bond formation and exclude hydrolysis of peptidyl-tRNA. Nature. 2005; 438:520–524. [PubMed: 16306996]
12. Voorhees RM, Weixlbaumer A, Loakes D, Kelley AC, Ramakrishnan V. Insights into substrate stabilization from snapshots of the peptidyl transferase center of the intact 70S ribosome. Nat Struct Mol Biol. 2009
13. Lancaster LE, Savelsbergh A, Kleanthous C, Wintermeyer W, Rodnina MV. Colicin E3 cleavage of 16S rRNA impairs decoding and accelerates tRNA translocation on Escherichia coli ribosomes. Mol Microbiol. 2008; 69:390–401. [PubMed: 18485067]
14. Nomoto S, Shiba T. Chemical Studies on Tuberactinomycin .13. Modification of Beta-Ureidodehydroalanine Residue in Tuberactinomycin-N. Journal of Antibiotics. 1977; 30:1008–1011. [PubMed: 591454]
15. Yamada T, Teshima T, Shiba T. Activity of di-beta-lysyl-capreomycin IIA and palmitoyl tuberactinamine N against drug-resistant mutants with altered ribosomes. Antimicrob Agents Chemother. 1981; 20:834–836. [PubMed: 6173016]
16. von Nussbaum F, Brands M, Hinzen B, Weigand S, Habich D. Antibacterial Natural Products in Medicinal Chemistry — Exodus or Revival? Angewandte Chemie. 2006; 45:5072–5129. [PubMed: 16881035]
17. Monshupanee T, Gregory ST, Douthwaite S, Chungjatupornchai W, Dahlberg AE. Mutations in conserved helix 69 of 23S rRNA of Thermus thermophilus that affect capreomycin resistance but not posttranscriptional modifications. J Bacteriol. 2008; 190:7754–7761. [PubMed: 18805973]
18. Schuwirth BS, et al. Structures of the bacterial ribosome at 3.5 Å resolution. Science. 2005; 310:827–834. [PubMed: 16272117]
19. Ali IK, Lancaster L, Feinberg J, Joseph S, Noller HF. Deletion of a conserved, central ribosomal intersubunit RNA bridge. Mol Cell. 2006; 23:865–874. [PubMed: 16973438]
20. Kipper K, Hetenyi C, Sild S, Remme J, Liiv A. Ribosomal intersubunit bridge B2a is involved in factor-dependent translation initiation and translational processivity. J Mol Biol. 2009; 385:405–422. [PubMed: 19007789]
21. O'Connor M. Helix 69 in 23S rRNA modulates decoding by wild type and suppressor tRNAs. Mol Genet Genomics. 2009
22. Borovinskaya MA, et al. Structural basis for aminoglycoside inhibition of bacterial ribosome recycling. Nat Struct Mol Biol. 2007; 14:727–732. [PubMed: 17660832]
23. Mears JA, et al. Modeling a minimal ribosome based on comparative sequence analysis. J Mol Biol. 2002; 321:215–234. [PubMed: 12144780]
24. Selmer M, et al. Structure of the 70S ribosome complexed with mRNA and tRNA. Science. 2006; 313:1935–1942. [PubMed: 16959973]
25. Weixlbaumer A, et al. Crystal structure of the ribosome recycling factor bound to the ribosome. Nat Struct Mol Biol. 2007; 14:733–737. [PubMed: 17660830]
26. Laurberg M, et al. Structural basis for translation termination on the 70S ribosome. Nature. 2008; 454:852–857. [PubMed: 18596689]
27. Korostelev A, et al. Crystal structure of a translation termination complex formed with release factor RF2. Proc Natl Acad Sci U S A. 2008; 105:19684–19689. [PubMed: 19064930]

28. Weixlbaumer A, et al. Insights into translational termination from the structure of RF2 bound to the ribosome. Science. 2008; 322:953–956. [PubMed: 18988853]
29. Moazed D, Noller HF. Intermediate states in the movement of transfer RNA in the ribosome. Nature. 1989; 342:142–148. [PubMed: 2682263]
30. Agirrezabala X, et al. Visualization of the hybrid state of tRNA binding promoted by spontaneous ratcheting of the ribosome. Mol Cell. 2008; 32:190–197. [PubMed: 18951087]
31. Kim HD, Puglisi JD, Chu S. Fluctuations of transfer RNAs between classical and hybrid states. Biophys J. 2007; 93:3575–3582. [PubMed: 17693476]
32. Pan D, Kirillov SV, Cooperman BS. Kinetically competent intermediates in the translocation step of protein synthesis. Mol Cell. 2007; 25:519–529. [PubMed: 17317625]
33. Ermolenko DN, et al. The antibiotic viomycin traps the ribosome in an intermediate state of translocation. Nat Struct Mol Biol. 2007; 14:493–497. [PubMed: 17515906]
34. Cornish PV, Ermolenko DN, Noller HF, Ha T. Spontaneous intersubunit rotation in single ribosomes. Mol Cell. 2008; 30:578–588. [PubMed: 18538656]
35. Zhang W, Dunkle JA, Cate JH. Structures of the ribosome in intermediate states of ratcheting. Science. 2009; 325:1014–1017. [PubMed: 19696352]
36. Shoji S, Walker SE, Fredrick K. Ribosomal Translocation: One Step Closer to the Molecular Mechanism. ACS Chem Biol. 2009
37. Peske F, Savelsbergh A, Katunin VI, Rodnina MV, Wintermeyer W. Conformational changes of the small ribosomal subunit during elongation factor G-dependent tRNA-mRNA translocation. J Mol Biol. 2004; 343:1183–1194. [PubMed: 15491605]
38. Carter AP, et al. Functional insights from the structure of the 30S ribosomal subunit and its interactions with antibiotics. Nature. 2000; 407:340–348. [PubMed: 11014183]
39. Borovinskaya MA, Shoji S, Fredrick K, Cate JH. Structural basis for hygromycin B inhibition of protein biosynthesis. Rna. 2008; 14:1590–1599. [PubMed: 18567815]
40. Szaflarski W, et al. New features of the ribosome and ribosomal inhibitors: non-enzymatic recycling, misreading and back-translocation. J Mol Biol. 2008; 380:193–205. [PubMed: 18508080]

Methods

41. Mayer C, RajBhandary UL. Conformational change of Escherichia coli initiator methionyl-tRNA(fMet) upon binding to methionyl-tRNA formyl transferase. Nucleic Acids Res. 2002; 30:2844–2850. [PubMed: 12087168]
42. Blaha G, Stanley RE, Steitz TA. Formation of the first peptide bond: the structure of EF-P bound to the 70S ribosome. Science. 2009; 325:966–970. [PubMed: 19696344]
43. Perona JJ, Swanson R, Steitz TA, Soll D. Overproduction and purification of Escherichia coli tRNA(2Gln) and its use in crystallization of the glutaminyl-tRNA synthetase-tRNA(Gln) complex. Journal of Molecular Biology. 1988; 202:121–126. [PubMed: 2459391]
44. Kabsch, W. XDS. In: Rossmann, MG.; Arnold, E., editors. International Tables in Crystallography. Vol. Vol. F. Dordrecht, Netherlands: Published for the International Union of Crystallography by Springer; 2005. p. 730-734.
45. McCoy AJG-K, R.W. Adams PD, Winn MD, Storoni LC, Read RJ. Phaser crystallographic software. J Appl Cryst. 2007; 40:658–674. [PubMed: 19461840]
46. Murshudov GN, Vagin AA, Dodson EJ. Refinement of macromolecular structures by the maximum-likelihood method. Acta Crystallogr D Biol Crystallogr. 1997; 53:240–255. [PubMed: 15299926]
47. Adams PD, et al. PHENIX: building new software for automated crystallographic structure determination. Acta Crystallogr D Biol Crystallogr. 2002; 58:1948–1954. [PubMed: 12393927]
48. Emsley P, Cowtan K. Coot: model-building tools for molecular graphics. Acta Crystallogr D Biol Crystallogr. 2004; 60:2126–2132. [PubMed: 15572765]
49. Brunger AT. Version 1.2 of the Crystallography and NMR system. Nat Protoc. 2007; 2:2728–2733. [PubMed: 18007608]

50. Brunger AT, et al. Crystallography & NMR system: A new software suite for macromolecular structure determination. Acta Crystallogr D Biol Crystallogr. 1998; 54:905–921. [PubMed: 9757107]

51. Bycroft BW. Crystal-Structure of Viomycin, a Tuberculostatic Antibiotic. Journal of the Chemical Society-Chemical Communications. 1972 660-&.

52. Yoshioka H, et al. Chemical Studies on Tuberactinomycin .2. Structure of Tuberactinomycin-O. Tetrahedron Letters. 1971 2043-&.

53. Bowers, K.; Chow, E.; Xu, H.; Dror, RO.; Eastwood, MP. Scalable Algorithms for Molecular Dynamics Simulations on Commodity Clusters. Proceedings of the ACM/IEEE Conference on Supercomputing (SC06); Tampa, Florida. 2006.

54. Jorgensen WL, Maxwell DS, TiradoRives J. Development and testing of the OPLS all-atom force field on conformational energetics and properties of organic liquids. Journal of the American Chemical Society. 1996; 118:11225–11236.

55. Jorgensen WL, Chandrasekhar J, Madura JD, Impey RW, Klein ML. Comparison of Simple Potential Functions for Simulating Liquid Water. Journal of Chemical Physics. 1983; 79:926–935.

56. DeLano, WL. The PyMol Molecular Graphics System. Palo Alto, CA: DeLano Scientific; 2002.

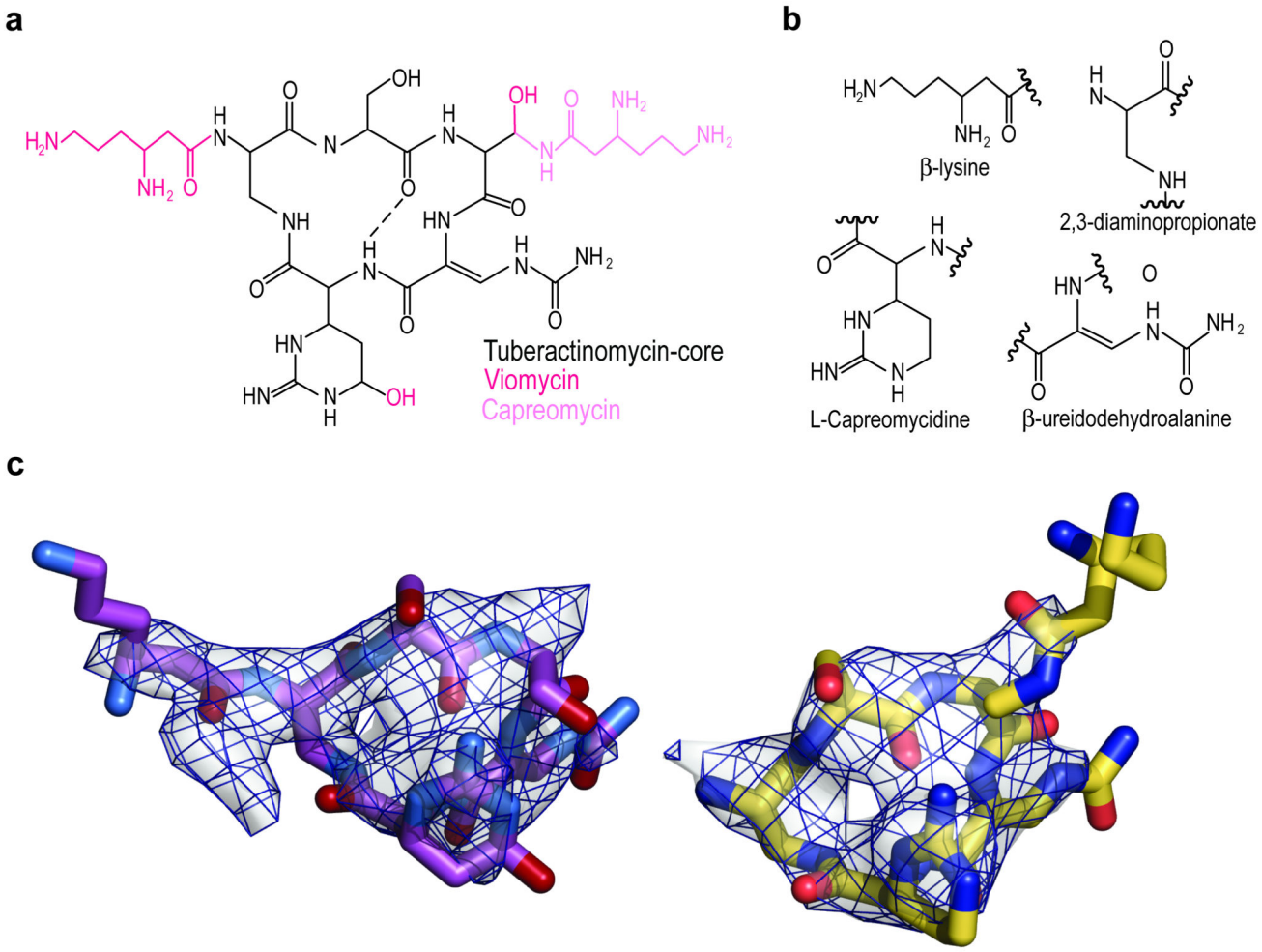

Figure 1.

Chemical Structure of the tuberactinomycins. (**a**) The chemical structures of viomycin and capreomycin IA. For simplicity only capreomycin IA is displayed. The other isoforms of capreomycin contain fewer functional groups (supplemental fig.1). The distinctive features of viomycin are in magenta and those of capreomycin are in pink. (**b**) Chemical structures of the unusual amino acids, from which the tuberactinomycins are built and which are referred to in the text. (**c**) Unbaised Fo-Fc difference Fourier map for viomycin and capreomyicn bound to a complex of T. thermophilus 70S, mRNA and tRNAs. The difference electron densities are contoured at 2.8 and 3.0 σ for viomycin (left) and capreomycin (right), and the refined models of viomycin (magenta) and capreomyicn (pink) are superimposed.

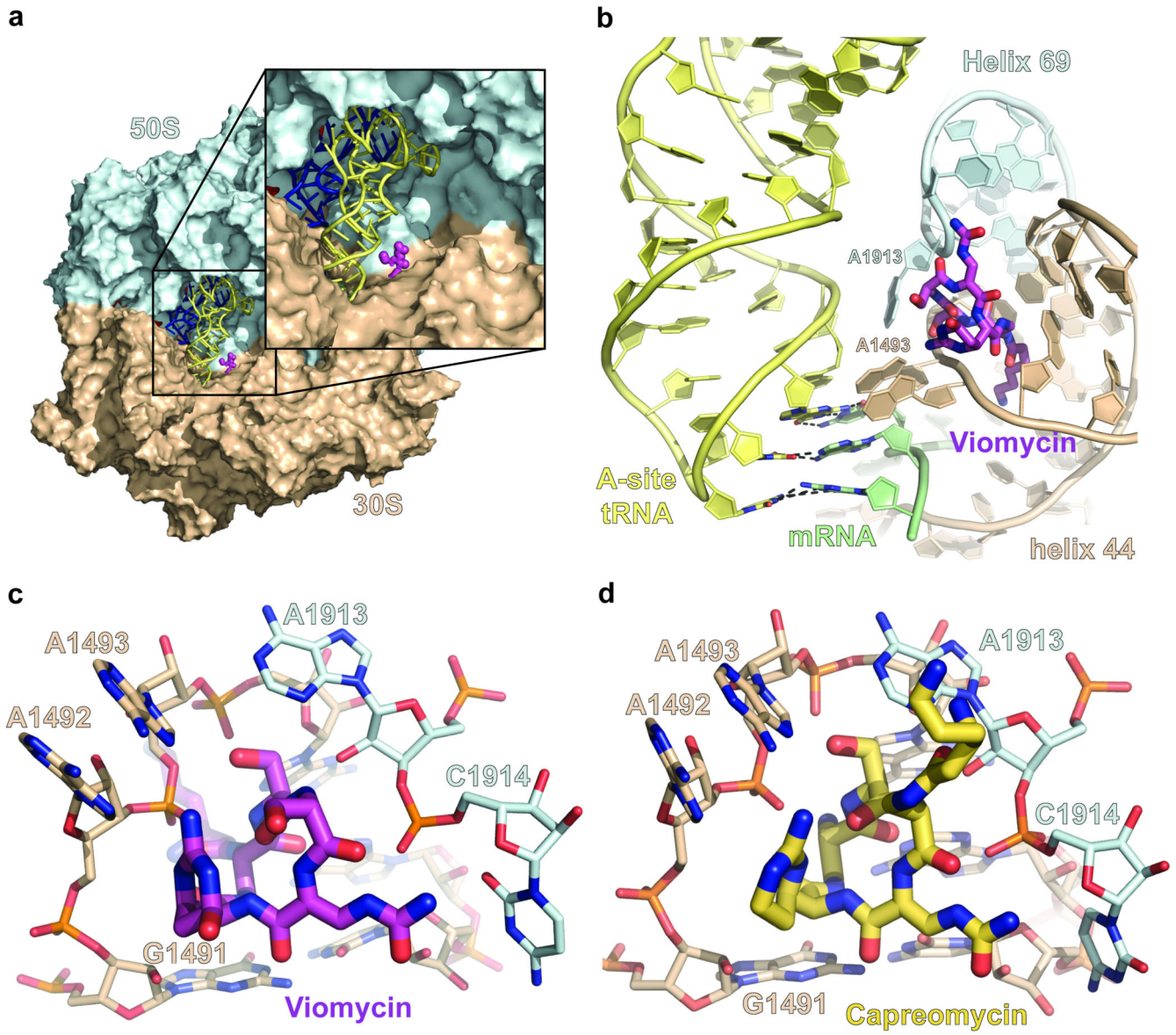

Figure 2.

Binding site of Viomycin and Capreomycin. (**a**) Overview of the entire structure of the ribosome complex with viomycin. Both the 50S ribosomal subunit (cyan) and the 30S ribosomal subunit (light brown) are shown in surface representation. The A-site tRNA (yellow) and the P-site tRNA (blue) are shown in ribbon, while viomycin (magenta) is shown as a spacefilled model. (**b**) Close up view of the viomycin binding site as shown in (a). The codon:anticodon base pairing between the A-site tRNA (yellow) and the mRNA (green) is indicated as black dashed lines. (**c**) Detailed view of the binding site of viomycin (magenta) illustrating its close proximity to A1492, A1493, and G1491 of h44 and A1913 and C1914 of H69. (**d**) Detailed view of the binding site of capreomycin (yellow) illustrating its close proximity to A1492, A1493, and G1491 of h44 and A1913 and G1941 of H69.

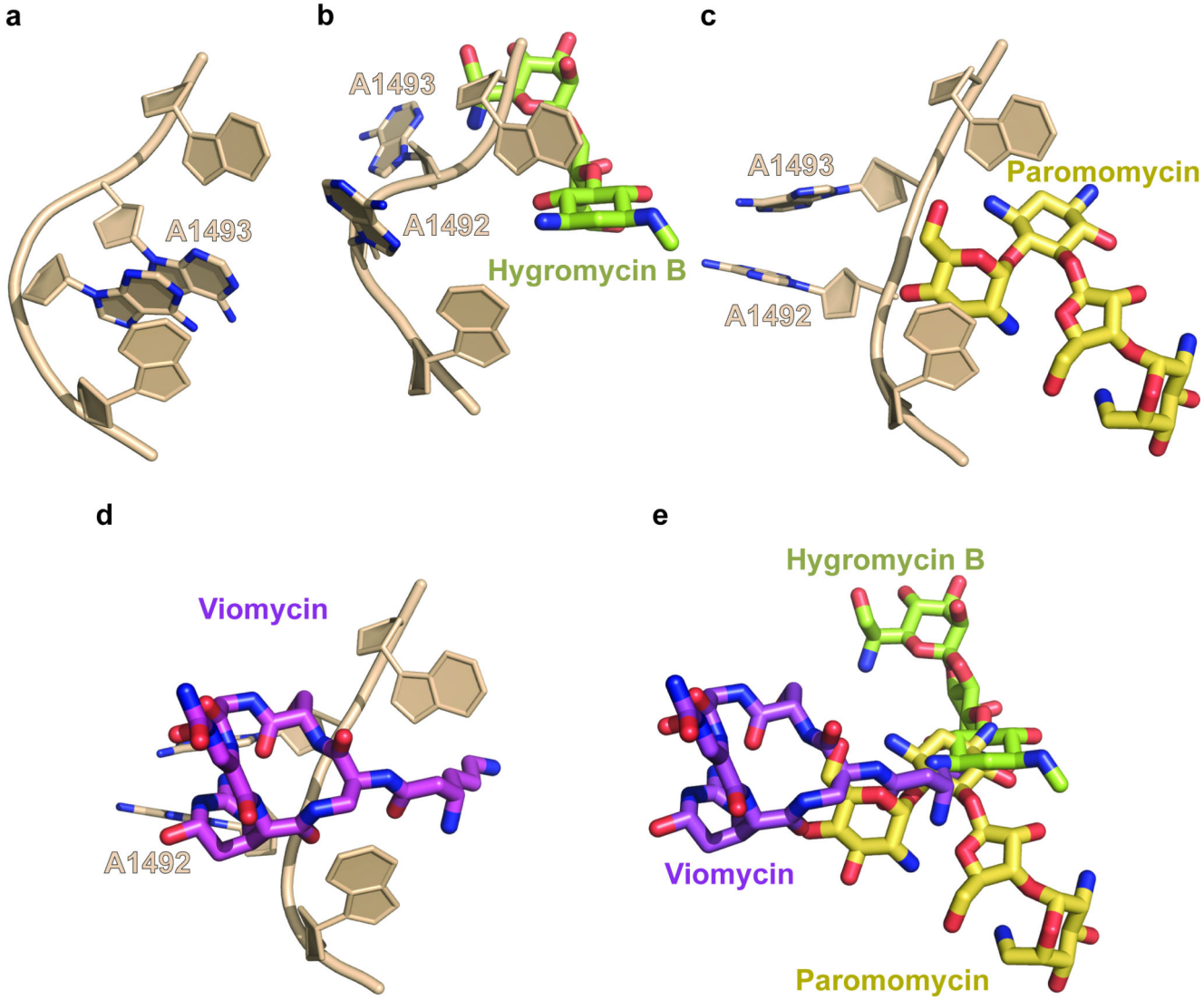

Figure 3.

Overlapping Binding Sites. (**a**) The region around 1492 and 1493 of h44 showing their base stacking in the apo 70S ribosome of *E. coli* (PDB ID 2AW4) 18. The nitrogens of the base of A1492 and A1493 are in blue and all other atoms are in light brown. (**b**) The binding site of hygromycin B showing the "flipped out" orientations of 1492 and 1493. The *carbons* of hygromycin are in green, the nitrogens in blue and the oxygens in red. The colour coding of the 16S rRNA is the same in (a). The coordinates were taken from PDB IDs 3DF1 39. (**c**) The binding site of paromomycin (yellow). The coordinates were taken from PDB ID 2WDG 12. (**d**) The binding site of viomycin (magenta) showing the same "flipped out" orientation of 1492 and 1493 as in (c). (**e**) Overlap of the binding sites of hygromycin B, paromomycin and viomycin. The superpositioning was based on h44 of the 16S rRNA with the exception of nucleotides A1492 and A1493.

Table 1

Data collection and refinement statistics (molecular replacement)

	Viomycin	Capreomycin
Data collection		
Space group	$P2_12_12_1$	$P2_12_12_1$
Cell dimensions		
a, *b*, *c* (Å)	210.2, 448.5, 633.6	210.4, 448.2, 631.2
α, β, γ (°)	90.0, 90.0, 90.0	90.0, 90.0, 90.0
Resolution (Å)	50 – 3.25 (3.3-3.25) *	50.0-3.5 (3.6-3.5) *
R_{sym} or R_{merge}	32.9 (120.9)	19.8 (60.7)
I / σI	4.2 (1.0)	5.6 (1.5)
I / σI= 2	3.5	3.6
Completeness (%)	99.5 (98.9)	82.0 (54.3)
Redundancy	3.7 (2.0)	4.6 (2.8)
Refinement		
Resolution (Å)	50 – 3.15	50 -3.5
No. reflections	1020688	661327
R_{work} / R_{free}	24.8 / 27.2%	23.3 / 27.01%
No. Atoms		
rRNA	189962	189171
r-protein	93456	93726
tRNA/mRNA/antibiotic/ion	12158	10879
B-factors	(Ask for input)	
r-RNA	83.2	75.7
r-protein	89.8	78.4
Ligand/ion	111.8	114.1
R.m.s. deviations		
Bond lengths (Å)	0.008	0.007
Bond angles (°)	1.42	1.27

* Values in parentheses are for highest-resolution shell.